

Morphology and Biometrics of the Vertebral Column, Ribs, and Sternum of the Collared Anteater

Adriana Gradela¹, Marcelo D. de Faria¹, Alisson J. de O. Nunes¹, Raphaela C. Torres¹, Fábio M. Corrêa²

¹Universidade Federal do Vale do São Francisco (Univasf), Petrolina, PE, Brazil.

²Department of Mathematical Statistics and Actuarial Sciences, University of the Free State, Bloemfontein, South Africa

Disclose and conflicts of interest: none to be declared by all authors

ABSTRACT

Introduction: the collared anteater (*Tamandua tetradactyla*) is considered an endangered species. Since morphological differences related to its territorial origins justify new research, the morphology and biometrics of the vertebral column, ribs, and sternum of the collared anteater were described and compared with the Xenarthra and mammals aiming to contribute to preservation measures, the clinical-surgical routine, and comparative studies. First, the vertebral columns from three adult carcasses were assembled after chemical maceration. Subsequently, the morphology and biometrics of the cervical (C), thoracic (T), lumbar (L), sacral (S), and caudal vertebrae (Ca), ribs (Co), and sternum were evaluated. The vertebral formula was C7 T16-17 L3 S5 Ca20-33= 50-64. Sixteen (67%) or 17 (33%) anteroposteriorly expanded pairs of ribs attached to their respective thoracic vertebrae were observed, whose number of sternal, asternal, and floating ribs were 10, 3, and 3 (33%), 11, 2, and 3 (33%), and 10, 4, and 3 (33%), respectively. The mammillary process occurred from T13 to L3, whereas the xenarthrous process occurred from L1 to L3. The sacrum was formed by the fusion from S1 to S5, with S1, S2, and part of S3 fused to the ilia and S5 to the ischia. The caudal vertebrae showed no spinous processes, and after Ca20 (33%) or Ca25 (33%), the transverse process originated in the caudal articular process. The results reveal that the collared anteater shows intra- and interspecific variations with other Xenarthra and mammals in the vertebral count, the location of the xenarthrous and haemal processes, and the absence of fusion in the vertebrae from the anterior part of the tail to the sacrum. Moreover, body weight support during the bipedal posture is performed by the xenarthrous processes of the lumbar vertebrae.

Keywords: *Tamandua tetradactyla*; Xenarthrous processes; Xenarthra; Lumbar vertebrae.

Introduction

The collared anteater (*Tamandua tetradactyla*), also known as maxilla, is found from Central to South America and east of the Andes¹. In Brazil, the species is found throughout the entire territory and features in regional lists as an endangered species² due to the habitat loss caused by predation by exotic species, deforestation for agricultural expansion, roadkill events, fires, attacks by domestic dogs, hunting, manufacturing of leather objects, or illegal trade for their inappropriate use as pets^{3,4}.

The collared anteater belongs to the superorder Xenarthra. Their specimens share particular anatomical features, e.g., other intervertebral joints (Xenarthrales or Xenarthrous process) observed in the caudal thoracic vertebrae and lumbar vertebrae⁵. In the Xenarthra, the vertebrae of the anterior part of the tail are fused to the sacrum, forming a synsacrum connected to the ilium through the sacroiliac joint and to the ischium through the sacro-ischiadic suture⁶, well-developed and ossified sternocostal joints and smaller teeth⁷. There is also a relatively high variation in the thoracolumbar vertebral count⁸.

The collared anteater shows morphological differences related to its territorial origin³. Moreover,

there are few reports on its body morphology and none on the biometric evaluation of its spinal bones, highlighting the relevance of this study in the field of morphological sciences. Therefore, this study aimed to describe the morphological and biometric characteristics of the vertebral column, ribs, and sternum of the collared anteater (*T. tetradactyla*) by comparing them with mammals and the Xenarthras, contributing to preservation measures, the clinical-surgical routine, and comparative studies.

Materials and Methods

Animals

The Research Ethics Committee approved this study of Universidade Federal do Vale do São Francisco (UNIVASF) under protocol No. 08121017. The skeletons of three adult collared anteaters (*T. tetradactyla*) belonging to the Didactic Museum of Animal Anatomy of the Federal University of Vale do São Francisco (UNIVASF) were assembled using roadkill carcasses obtained from highways of the state of Pernambuco. The authors state that every effort was made to follow all local and international ethical guidelines and laws that pertain to the use of human cadaveric donors in anatomical research⁹. The skeletons' preparation,

storage, and dissection occurred in the Laboratory of Domestic and Wild Animal Anatomy of UNIVASF. First, the carcasses were eviscerated, and the flesh was manually removed using knives, scalpels, and tweezers. Next, the vertebrae and ribs were tied with strings to maintain their order, and the soft tissues attached to the bones were removed by quick maceration through boiling for three hours. After their removal, the bones were cleaned with 16.0 cm anatomical tweezers and 15.0 cm straight blunt and curved blunt scissors until the complete removal of soft tissues. Subsequently, the bones were bleached in 15% hydrogen peroxide for about four hours, washed in running water, sun-dried, and articulated using galvanized steel wires.

Anatomical and biometric study of the ribs, vertebral column, and sternum

The morphological description of the ribs (Co), thoracic (T), lumbar (L), sacral (S), caudal vertebrae (Ca) and sternum followed the nomenclature proposed by the International Committee on Veterinary Gross Anatomical Nomenclature (NAV 2012). The bones from each spinal segment were quantified, and the length (cm), width (cm), and height (cm) were measured using a millimetre calliper (Starret 125MEB). The ribs were also evaluated for thickness (cm). The discoveries were photographically documented using a digital camera (Sony DSC-H50, Brazil).

Statistical Analysis

The data were subjected to analysis of variance (ANOVA) and Scott-Knott test ($p < 0.05$). The analyses were performed with the software R.4.2.1.

Results

The vertebral formula obtained was $C_7 T_{16-17} L_3 S_5 Ca_{20-33} = 50-64$. All specimens showed an equal number of ribs and thoracic vertebrae.

Cervical vertebrae

The first two cervical vertebrae, C1 (atlas) and C2 (axis) had different morphologies (Figure 1). The body of the atlas had a ventral arch to connect with the odontoid process of the axis and, laterally, a wing. Its cranial part articulated with the occipital condyles, and the caudal part had a fovea that articulated with the axis and showed lateral, transverse, and alar vertebral foramina. The axis showed the odontoid process, two small transverse processes projected caudally containing foramina, and a broad and robust spinous process. C1 showed a significantly longer length of the transverse process ($p < 0.05$) than the other vertebrae (Table 1).

Thoracic cage or rib cage

The rib cage was formed by the junction of ribs, sternum, and costal cartilages. The sternum was an odd, long, dorsoventrally flattened, caudally inclined

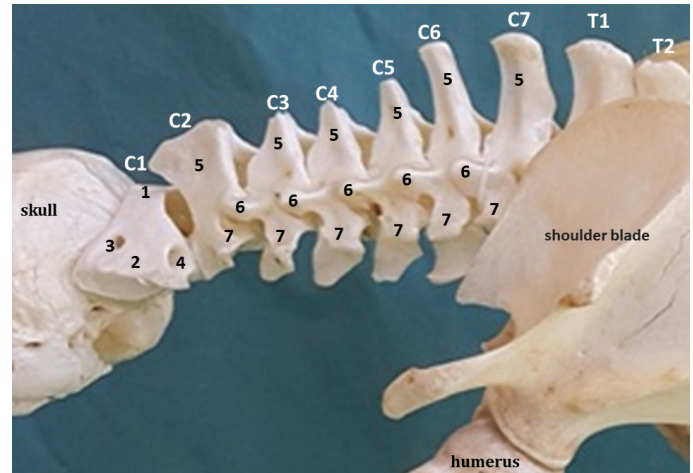


Figure 1. Lateral view of the cervical spine of an adult collared anteater (*T. tetradactyla*), Petrolina/PE, 2019. Atlas (C1), axis (C2), and remaining cervical vertebrae (C3-C7), dorsal tubercle, wing (2), alar and lateral vertebral foramina (3), transverse foramen (4), spinous processes (5), articular processes (6), and transverse process (7).

Table 1. Mean \pm standard error of the mean of the cervical spine vertebrae (C) of adult collared anteaters (*T. tetradactyla*) in Petrolina/PE.

No	Body			S.P.	L.T.P.
	Length (cm)	Width (cm)	Height (cm)	Height (cm)	Length (cm)
C1	1.53 \pm 0.46	2.40 \pm 0.53	1.47 \pm 0.18	0.77 \pm 0.63	1.17 \pm 0.18 ^a
C2	1.50 \pm 0.80	1.80 \pm 0.80	1.83 \pm 1.23	0.63 \pm 0.88	0.87 \pm 0.77 ^b
C3	1.33 \pm 1.27	1.87 \pm 1.23	1.90 \pm 1.22	0.57 \pm 0.93	0.67 \pm 0.63 ^b
C4	0.97 \pm 0.63	2.07 \pm 0.98	2.03 \pm 1.37	0.50 \pm 0.30	0.60 \pm 0.53 ^b
C5	1.03 \pm 0.93	2.10 \pm 1.10	2.07 \pm 1.56	0.83 \pm 0.93	0.63 \pm 0.46 ^b
C6	1.03 \pm 0.46	2.33 \pm 0.88	2.43 \pm 1.23	0.87 \pm 0.77	0.70 \pm 0.80 ^b
C7	0.90 \pm 0.00	2.27 \pm 0.77	1.97 \pm 1.07	0,87 \pm 1,15	0.67 \pm 0.77 ^b

Averages followed by the same lowercase letter on the same column did not differ significantly ($P < 0.05$) by the Scott-Knott test.

bone located ventrally in the rib cage and attached to the vertebral column through the ribs, which provided high stability. The bone showed a broad, wide, and oval manubrium (presternum), a body (mesosternum) consisting of eight or nine short segments (sternebrae) wider dorsally, from which emerged a process in the shape of an inverted club and ossified from a main sternal centre, and a very long and simple xiphisternum (Figure 2).

Morphologically, the ribs consisted of a body and two ends, with the body varying in length, width, and thickness. The vertebral end of the rib consisted of a head articulated with the bodies of the thoracic vertebrae, a neck joining the head to the body, and a tubercle located caudal to the head and articulated with the transverse processes of the thoracic vertebrae. The head of each rib consisted of a slightly squared bone surface on the proximal epiphysis, with a flat facet connected at the fovea to the head of the rib of each thoracic vertebra, forming a flat synovial joint. The ventral ends of each rib were broad and wrinkled at the costochondral junction. The first rib was shorter, while the last was thinner (Figure 2).

The ribs, totalling 16 (67%) or 17 (33%), were even, anteroposteriorly expanded, and each pair was attached to their respective thoracic vertebra. Part of the head of the first rib was held by the body of the last cervical vertebra, whereas the remaining ribs were connected only to their corresponding thoracic vertebra. The proportion of true or sternal ribs, false or asternal ribs, and floating ribs were 10, 3, and 3 (N = 33%), 11, 2, and 3 (33%), and 10, 4, and 3 (33%), respectively. The ribs showed the longest length in Co9 and Co13 and the shortest in Co1; the greatest width in Co1 and the smallest in Co3, Co14 and Co15, and the greatest thickness in Co9 and Co10 and the smallest in Co5 (Table 2).

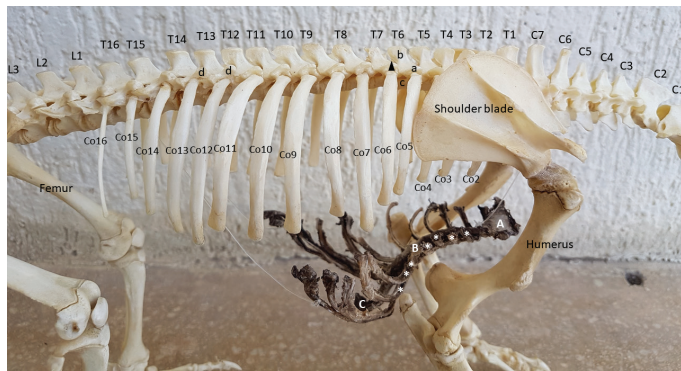


Figure 2. Rib cage and vertebrae of the cervical (C1-C7), thoracic (T1 to T16) and lumbar (L1-L3) spine of an adult collared anteater (*T. tetradactyla*), Petrolina/PE, 2019. (A) manubrium, (B) body and (C) xiphoid cartilage of the sternum, (*) segments with articular facets for the sternal ribs; (Co) rib; (a) transverse process, (b) spinous process, (c) body, (triangle) costal fovea of the transverse process, and (d) mammillary process of the thoracic vertebrae.

Table 2. Rib dimensions (mean + standard error of the mean) of adult collared anteaters (*T. tetradactyla*) in Petrolina/PE.

Rib Number	Length	Width	Thickness
Co1	2.27±1.23 ^a	0.70±1.10 ^a	0.30±0.53 ^a
Co2	2.67±2.07 ^b	0.60±0.30 ^b	0.27±0.18 ^b
Co3	3.00±2.41 ^b	0.47±0.46 ^c	0.27±0.46 ^b
Co4	3.33±2.48 ^a	0.53±0.35 ^b	0.33±0.46 ^a
Co5	3.87±2.89 ^a	0.60±0.91 ^b	0.23±0.35 ^a
Co6	3.93±2.62 ^a	0.53±0.63 ^b	0.30±0.00 ^a
Co7	4.50±2.41 ^a	0.53±0.46 ^b	0.27±0.18 ^a
Co8	4.40±2.19 ^a	0.50±0.61 ^c	0.30±0.00 ^a
Co9	4.83±2.83 ^a	0.57±0.46 ^b	0.37±0.18 ^a
Co10	4.80±2.49 ^a	0.57±0.46 ^b	0.37±0.18 ^a
Co11	4.70±2.13 ^a	0.60±0.30 ^b	0.33±0.18 ^a
Co12	4.73±2.03 ^a	0.53±0.18 ^b	0.33±0.18 ^a
Co13	4.83±1.93 ^a	0.57±0.18 ^b	0.30±0.30 ^a
Co14	4.47±1.56 ^a	0.47±0.35 ^c	0.33±0.18 ^a
Co15	3.60±2.63 ^b	0.47±0.18 ^c	0.27±0.18 ^b
Co16	2.75±2.29 ^b	0.30±0.00 ^d	0.25±0.90 ^b

Averages followed by the same lowercase letter on the same column did not differ significantly (P<0.05) by the Scott-Knott test.

Thoracic vertebrae

The thoracic vertebrae differed from the cervical ones by the presence of an articular facet for the ribs, consisting of a body, a dorsally projected spinous process, two transverse processes emerging laterally from each antimer, and a vertebral foramen. Mammillary processes were observed from T13 to T16-17, and the spinous processes were inclined caudally from T1 (Figure 2). Sixteen (67%) or 17 (33%) thoracic vertebrae were observed, and the length and width of the transverse processes were shown (Table 3). In the body, the width was greater than the length and height, and these variables did not change significantly (p > 0.05) between vertebrae, except for the decrease (p < 0.05) in height observed from T2 to T10.

Lumbar vertebrae

Three lumbar vertebrae were observed in 100% of the animals and consisted of a body, a vertebral foramen, a spinous process, two transverse processes, and two xenarthrous processes. The mammillary processes were as developed as those of the thoracic vertebrae. They showed concave facets turned to the median plane, with their ventral base articulating with the previous vertebra's dorsal and ventral xenarthrous processes (Fig.3). The vertebrae had a uniform shape, and the body was long and cylindrical, with the width greater than the height, which, in turn, was greater than the length. The measures were equivalent to those of the thoracic vertebrae. The transverse processes were longer and broader than the spinous processes. They had an equivalent height and width about the thoracic vertebrae, caudal inclination, and uniform height from L1 to L3 (Table 4).

Sacrum

The sacrum was a single bone formed by the fusion of five vertebrae (S1 to S5) whose transverse processes were fused in a single bone and consisted of a body traversed by a single vertebral canal. The bone had a caudally enlarged rectangular shape caused by the prolongation of the transverse processes of S5, with the caudal end being slightly more raised than the cranial end. The sacrum had two surfaces, two edges, one base (cranial), and one apex (caudal). The middle portion of the base comprised the head of S1, slightly protruding and transversally elongated. The base of the transverse processes was fused, very thick, vertically raised, transversally concave, and slightly convex dorsoventrally. S5 articulated with Ca1 in the apex showed a very long and caudally projected transverse process (Figure 4). On the median plane, the dorsal surface showed a series of five sacral spinous processes more or less fused and slightly inclined caudally, forming the lateral sacral crest, ventrally to which there were four dorsal sacral foramina in both antimeres. The pelvic surface helped form the dorsal wall of the pelvic cavity was concave in the

Table 3. Mean + standard error of the mean of the thoracic vertebrae of adult collared anteaters (*T. tetradactyla*) in Petrolina/PE.

Nº	Body			Spinous Process		Transverse Process	
	Length	Width	Height	Height	Width	Length	Width
T1	0.77±0.18	2.10±0.91	1.87±0.63 ^a	0.77±1.15	0.80±1.10	0.53±0.18	0.77±0.63
T2	0.73±0.18	2.17±0.77	1.67±1.27 ^b	0.63±0.98	0.63±0.63	0.60±0.53	0.87±0.46
T3	0.77±0.18	2.07±0.46	1.73±0.63 ^b	0.60±0.53	0.63±0.18	0.63±0.70	0.90±0.53
T4	0.73±0.18	2.10±0.61	1.60±0.80 ^b	0.60±0.53	0.63±0.35	0.67±0.63	0.83±0.63
T5	0.80±0.00	1.97±0.77	1.60±0.61 ^b	0.60±0.53	0.63±0.18	0.63±0.35	0.83±0.77
T6	0.83±0.18	2.07±0.70	1.63±0.46 ^b	0.60±0.80	0.53±0.35	0.60±0.30	0.93±0.88
T7	0.83±0.18	2.10±0.53	1.63±0.63 ^b	0.60±0.80	0.57±0.46	0.57±0.18	0.97±0.70
T8	0.83±0.46	2.03±0.35	1.70±0.80 ^b	0.63±0.63	0.73±0.46	0.57±0.18	0.90±0.80
T9	0.80±0.30	2.10±0.53	1.77±0.70 ^b	0.70±0.61	0.73±0.46	0.63±0.18	0.83±0.63
T10	0.83±0.46	2.17±0.18	1.73±1.15 ^b	0.73±0.63	0.60±0.30	0.67±0.18	0.93±0.93
T11	0.80±0.30	2.07±0.46	1.87±0.70 ^a	0.73±0.63	0.63±0.18	0.63±0.18	0.90±0.80
T12	0.83±0.35	2.00±0.53	1.83±0.63 ^a	0.73±0.46	0.63±0.18	0.73±0.46	0.87±0.77
T13	0.87±0.46	1.93±0.18	1.90±0.53 ^a	0.70±0.61	0.53±0.46	0.80±0.53	1.00±0.80
T14	0.87±0.46	2.00±0.30	1.93±0.88 ^a	0.67±0.70	0.50±0.00	0.97±0.63	0.93±0.77
T15	0.77±0.18	2.20±1.10	1.97±0.70 ^a	0.57±0.70	0.53±0.18	1.17±0.77	1.07±1.07
T16	0.90±0.00	2.25±0.70	1.85±0.49 ^a	0.65±0.90	0.60±0.00	1.15±2.70	0.90±1.80

Averages followed by the same lowercase letter on the same column did not differ significantly (P<0.05) by the Scott-Knott test.

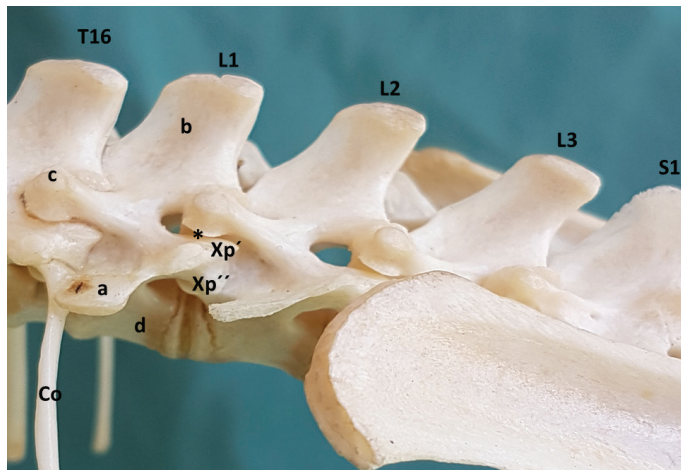


Figure 3. Lateral view of the lumbar (L) vertebrae of an adult collared anteater (*T. tetradactyla*), Petrolina/PE, 2019. (T16) sixteenth thoracic vertebra, (Co) rib, (S1) sacral vertebra, (a) transverse process, (b) spinous process, (c) mammillary process, (d) body, (*) joint processes, (Xp') dorsal xenarthrous process, (Xp'') ventral xenarthrous process.

was 2.10±0.80 cm. There was an increase (p<0.05) in the body width of S5, whereas the width of the right and left transverse processes decreased (p<0.05) in S2, increasing again (p<0.05) in S5 (Table 5).

Caudal vertebrae

The caudal vertebrae (Ca) showed significant variation in shape. Ca1 showed a slightly longer cranial articular process than the remainder since it articulated with the sacrum. All vertebrae showed a rounded vertebral body traversed by a vertebral canal, which opened through the vertebral foramen,

Table 4. Mean + standard error of the mean of the lumbar vertebrae of adult collared anteaters (*T. tetradactyla*) in Petrolina/PE.

	L1	L2	L3
Body Length	0.80 ± 0.53	0.87 ± 0.46	1.00 ± 0.80
Body width	2.53 ± 1.27	2.70 ± 0.80	2.77 ± 0.35
Body height	2.00 ± 0.61	2.07 ± 0.77	2.03 ± 0.77
Spinous process height	0.60 ± 0.30	0.60 ± 0.61	0.60 ± 0.61
Spinous process width	0.63 ± 0.18	0.60 ± 0.30	0.57 ± 0.18
Right transverse process Length	1.27 ± 0.63	1.03 ± 0.18	1.20 ± 0.30
Right transverse process width	1.27 ± 1.15	1.37 ± 0.88	1.33 ± 0.77
Left transverse process Length	1.40 ± 0.00	1.17 ± 0.70	1.20 ± 0.30
Left transverse process width	1.23 ± 1.23	1.27 ± 0.88	1.23 ± 1.07

craniocaudal direction and had ventral sacral foramina to allow the exit of the ventral sacral nerve roots. The cranially directed base was large and slightly narrower caudally. The union between the head of S1 and the last lumbar vertebra, L3, formed a projection angle ventral to the promontory and into the pelvic cavity. Sacral vertebrae were fused to the pelvis, with S1, S2, and part of S3 fused to the ilia and S5 to the ischia. The mean length of the sacrum was 5.90±2.20 cm, the mean width was 4.40±1.60 cm, and the mean height

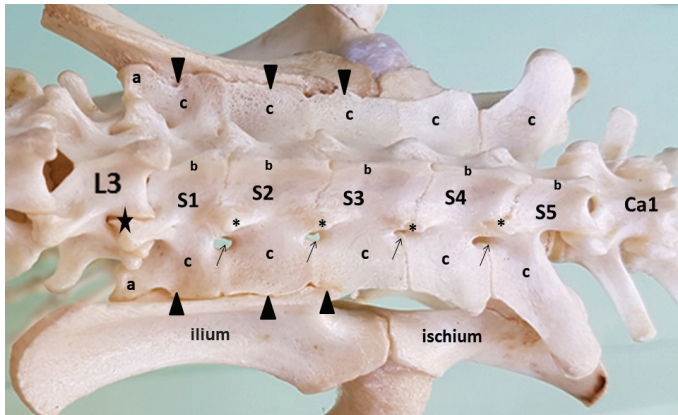


Figure 4. Dorsal view of the sacrum (S1 to S5) of an adult collared anteater (*T. tetradactyla*), Petrolina/PE, 2019. (a) wing, (b) spinous process, (c) lateral crest, (*) lateral crest, (star) joint of L3 with S1 and of S5 with Ca1, (black arrow) dorsal sacral foramina, (triangle) sacroiliac joint, and (Ca) caudal vertebra.

gradually decreasing in size until the end of the tail. No spinous processes were observed, and the transverse processes were also absent from Ca20 (33%) and Ca25 (33%) as they curved caudally and fused to the body, becoming caudal articular processes. Twenty (33%), 22 (33%), or 30 (33%) caudal vertebrae were observed, whose body length increased steadily until more or less half of the tail, then decreased until the last two vertebrae.

In contrast, the width decreased steadily from the first to the last vertebrae, and the height increased slightly around Ca5 and then decreased steadily until the last vertebra (Table 6). The length of the transverse process decreased and increased until Ca24, then disappeared from Ca25, whereas the width decreased steadily until Ca24 and then disappeared at Ca25 (Table 6). The haemal process was present in all caudal vertebrae from Ca1 and showed a “Y” shape.

Discussion

The study of the adult morphology of the vertebral column is essential to evaluate the embryological and molecular aspects of evolution since the number of vertebrae is directly coupled with the number of somites¹⁰. The results of this study were compared with findings for mammals, in general, and other Xenarthras since the literature is scarce regarding the collared anteater (*T. tetradactyla*). The spinous and transverse processes were common to all vertebrae except for the vertebrae caudal and the mammillary processes in the thoracic and lumbar¹¹.

The vertebral formula of the collared anteater diverged from the one previously presented for this species in relation to the thoracic (T17-18), lumbar (L2-3), sacral (S5-6), and caudal vertebrae (Ca24-37)^{12,6}. Compared to other species of the same Order, the vertebral formula of the collared anteater contrasted with that of the giant anteater about the sacral (S3-5) and caudal vertebrae (Ca23-27)¹³, or the lumbar (L2-3), sacral (S4-5), and caudal vertebrae (Ca23-27)⁵. It also contrasted with the northern tamandua to the

thoracic (T17-18) and lumbar vertebrae (L2)¹⁰, with the nine-banded armadillo about the lumbar (L4) and caudal vertebrae (Ca1)¹⁴ or the thoracic (T10), lumbar (L5), sacral (S9), and caudal vertebrae (Ca20-7)⁶, and with the silky anteater and Hoffmann's two-toed sloth in relation to the lumbar (L1-2), sacral (S4), and caudal vertebrae (Ca40)¹² or to all vertebrae¹⁵.

The cervical and caudal vertebrae's more significant difference and complexity¹⁶, and all vertebrae were free and unfused⁶ agreeing with previous studies. About morphology, the spinous processes were more robust on the caudal cervical vertebrae, as in the two-toed sloth¹⁷. The length of the spinous processes did not change between the cervical, thoracic, and lumbar spine of the collared anteater, unlike the dog, in which these structures are enlarged until the middle of the thoracic region and then decrease gradually¹¹, and the northern tamandua, which shows uniformly high and craniocaudally elongated spinous processes in the thoracic spine¹⁸. C1 led the most prominent transverse processes of the entire vertebral column, except for T15 to T16, L1 to L3, and S1 and S4 to S5, contrasting with the giant anteater¹³. Their transverse processes are more prominent on the lumbar vertebrae. Similar to dogs¹⁹, the length of the transverse processes from C3 to T14 showed no significant change. In contrast, the spinous process of C2 showed the most apparent width of the entire vertebral column, as described for the giant anteater. On the other hand, the most prominent heights were observed in C6 and C7, contrasting with the giant anteater¹³.

The morphology of the sternum did not differ from the description made for *Myrmecophaga anteaters*. However, the manubrium and the number of sternbrae diverged from the nine-banded armadillo⁶. The shape and inclination of the sternum were similar to those of domestic animals, and the number of sternbrae was similar to that of the domestic dog and higher than those of horses, pigs, and bovines¹⁹.

Although the shape of the ribs was similar to some domestic animals, this parameter differed from the lower number observed in equines and the higher number observed in ruminants, dogs, and swine¹⁹. The fossorial habit explained the anteroposterior expansion of the ribs²⁰, which, along with the xenarthrous processes of the lumbar region, increase the stability of the thorax and, consequently, the stability of the vertebral column. The shape and articulation of the ribs with the thoracic vertebrae corroborated with the description made for this specie⁶. In contrast, unilateral floating ribs were not observed as in the giant anteater⁵. The apex of rib length, observed in Co9 and Co10, was close to that observed in bovines and equines (Co10 or Co11), whereas the width decreased steadily from T1 to T17, differing from bovines, whose width of most ribs increased significantly in the middle. Similar to equines, the smallest rib was the first, while the last was the thinnest²¹.

Table 5. Mean ± standard error of the mean of the dimensions of the sacral vertebra (S) of adult collared anteaters (*T. tetradactyla*) in Petrolina/PE.

Sacral Vertebrae	S1	S2	S3	S4	S5
Body					
Length	1.03±0.63	0.90±0.80	0.93±0.63	1.10±1.80	1.07±0.88
Width	2.60±0.80 ^b	2.50±0.80 ^b	2.33±0.63 ^b	2.50±5.39 ^b	3.40±1.85 ^a
Height	1.80±0.30	1.67±1.15	1.43±0.63	1.55±2.70	1.37±0.88
Spinous Process					
Height	0.63±0.77	0.77±0.77	0.73±0.88	0.80±0,00	0.57±0.70
Right Transverse Process					
Length	1.17±0.70	1.07 0.70	0.97±0.77	1,00±0.00	1.40±1.22
Width	1.13±0.93 ^a	0.77±0.35 ^b	0.73±0.46 ^b	0.95±4.49 ^b	1.43±0.46 ^a
Left Transverse Process					
Length	1.13±0.88	1,00±0.53	1.03±0.63	1.10±0,00	1.40±1.10
Width	1.10±0.61 ^a	0.77±0.18 ^b	0.83±0.77 ^b	0.80±3.59 ^b	1.43±0.70 ^a

Averages followed by the same lowercase letter on the same row did not differ significantly (P<0.05) by the Scott-Knott test.

Tabela 6: Mean ± standard error of the mean of the dimensions of the caudal vertebrae (Ca) of adult collared anteaters (*T. tetradactyla*) in Petrolina/PE.

Caudal Vertebrae	Body			Transverse Process	
	Length	Width	Height	Length	Width
Ca1	1.17 ± 0.40	3,17 + 0,70	1,57+0,45	0,63+ 0,45	1,13+ 0,52
Ca2	0.97 ± 0.21	2.40 ± 0.37	1.53 ± 0.42	0.40 ± 0.24	0.97 ± 0.45
Ca3	0.97 ± 0.32	2.23 ± 0.42	1.50 ± 0.42	0.43 ± 0.16	0.93 ± 0.4
Ca4	0.93 ± 0.29	2.20 ± 0.55	1.57 ± 0.90	0.47 ± 0.08	0.77 ± 0.32
Ca5	1.00 ± 0.37	1.97 ± 0.52	1.73 ± 1.44	0.63 ± 0.08	0.60 ± 0.24
Ca6	1.07 ± 0.21	1.83 ± 0.45	1.47 ± 0.90	0.73 ± 0.08	0.57 ± 0.32
Ca7	1.40 ± 0.55	2.05 ± 0.14	1.65 ± 1.52	0.70 ± 0.28	0.65 ± 0.14
Ca8	1.13 ± 0.62	1.67 ± 0.45	1.40 ± 0.77	0.70 ± 0.14	0.60 ± 0.37
Ca9	1.45 ± 0.69	1.75 ± 0.42	1.50 ± 1.66	0.80 ± 0.00	0.55 ± 0.42
Ca10	1.45 ± 0.42	1.65 ± 0.42	1.30 ± 1.39	0.85 ± 0.14	0.55 ± 0.14
Ca11	1.27 ± 0.65	1.43 ± 0.42	1.13 ± 0.62	0.77 ± 0.21	0.43 ± 0.29
Ca12	1.35 ± 0.69	1.55 ± 0.14	1.10 ± 1.11	0.85 ± 0.14	0.50 ± 0.00
Ca13	1.35 ± 0.69	1.45 ± 0.42	1.10 ± 1.11	0.80 ± 0.00	0.45 ± 0.14
Ca14	1.13 ± 0.62	1.17 ± 0.42	0.97 ± 0.56	0.70 ± 0.24	0.33 ± 0.16
Ca15	1.17 ± 0.62	1.23 ± 0.42	0.93 ± 0.58	0.70 ± 0.37	0.30 ± 0.24
Ca16	1.07 ± 0.56	1.00 ± 0.50	0.80 ± 0.42	0.77 ± 0.21	0.23 ± 0.16
Ca17	1.03 ± 0.52	1.00 ± 0.42	0.70 ± 0.42	0.67 ± 0.21	0.23 ± 0.16
Ca18	0.97 ± 0.45	0.97 ± 0.45	0.73 ± 0.21	0.70 ± 0.24	0.17 ± 0.08
Ca19	0.93 ± 0.52	0.97 ± 0.45	0.70 ± 0.28	0.63 ± 0.4	0.17 ± 0.08
Ca20	1.30 ± 0.55	1.05 ± 0.14	0.70 ± 0.83	0.75 ± 0.14	0.20 ± 0.00
Ca21	1.05 ± 0.14	1.15 ± 0.14	0.65 ± 0.42	0.75 ± 0.14	0.10 ± 0.00
Ca22	0.95 ± 0.14	0.85 ± 0.14	0.35 ± 0.14	0.75 ± 0.14	0.10 ± 0.00

Averages followed by the same lowercase letter on the same column did not differ significantly (P<0.05) by the Scott-Knott test.

The number of thoracic vertebrae observed in this study was similar to that reported for the other species⁵. Within the Mammalia, the Xenarthra show the greatest variation in the number of thoracolumbar vertebrae²² and, unlike domestic animals²¹ (Getty 1986) and the nine-banded armadillo⁶ and similar to the domestic dog²³ (Anderson & Anderson 1994), their thoracic vertebrae differ from the cervical ones by the length of the transverse processes or the height of the spinous processes. The length, width, and height of the body of the thoracic vertebrae did not change, differing from equines, in which these parameters decrease until the middle of the thoracic region and then increase gradually²¹.

The anticlinal vertebra is often used as the point of reference in diagnostic imaging studies and to understand the behavioral habits of the species since it affects the muscular advantage of the longitudinal spinal muscles for different movements and activities²³. Despite its importance, its exact definition and anatomic location diverge among authors. In the collared anteaters of this study, the anticlinal vertebra was not observed, agreeing with the giant anteater⁵ and the two-toed sloth²⁴, and contrasting with the northern tamandua¹⁸.

T13 to T16-17 were considered caudal thoracic vertebrae due to the presence of prominent mammillary processes since the anticlinal vertebra or the lumbarization of the thoracic vertebrae⁶ were not observed. The mammillary processes were observed until L3, unlike other Xenarthra, in which they went until S1¹⁸. The absence of lumbarization in the thoracic vertebrae diverged from other representatives of this order, e.g., the nine-banded armadillo, the giant anteater, and the two-toed sloth, which showed xenarthrous processes in the caudal and lumbar thoracic vertebrae⁵. This finding is very significant as it indicates that, in the collared anteater, body weight support during the bipedal posture is performed only by the xenarthrous processes of the lumbar vertebrae.

The uniform shape and size of the lumbar vertebrae agreed with the giant anteater¹³ and domestic animals, diverging from the latter to the vertebral bodies, the spinous processes, the gradual decrease in the vertebrae from L1 to L3; the cranial orientation, and the transverse processes increased in length in the first vertebrae and then decreased until the last vertebra¹⁹.

The presence of dorsal and ventral xenarthrous processes agreed with the nine-banded armadillo⁶ and the giant anteater⁵. However, unlike these species, they were present only in the lumbar vertebrae of the collared anteater. The articulation of the xenarthrous process with the ventral base of the mammillary process of the anterior vertebra was similar to that described for the giant anteater²⁴. According to these authors, the function of the xenarthrous vertebrae

varies with the species. It seems to be related to the bipedal posture assumed by the anteaters when destroying termite mounds and anthills or protecting from enemies with the anterior claws, which demands that the lumbar vertebrae support the body weight.

The collared anteater showed an equal number of sacral vertebrae to that described for the giant anteater⁵. Similar to the giant anteater, the sacrum was a single bone formed by the fusion of several vertebrae whose spinous processes were caudally inclined, forming the median sacral crest. However, the rectangular shape, the absence of caudal narrowing, the rudimentary wing, and the apex with a slight upward inclination diverged from these species. Moreover, the sacrum showed no independent spinous processes.

Although the Xenarthra commonly show a fusion of the vertebrae from the anterior portion of the tail to the sacrum, resulting in the formation of a synsacrum connected to the ilium and the ischium⁶, the collared anteater only showed a fusion of S1, S2, and part of S3 with the ilia and S5 with the ischia, without a fusion of the vertebrae from the anterior portion of the tail to the sacrum. Moreover, the findings diverged from the giant anteater, which showed a fusion with the ilia until S4 and S5 fused with the ischia, also involving Ca1⁵, and from the nine-banded armadillo, which has all sacral vertebrae and Ca1 fused to the pelvis⁶.

The disappearance of the transverse process agreed with the giant anteater; however, unlike this species, it occurred in the final third of the tail and not in its middle region¹³.

The presence of the haemal process diverged from the others⁶. Since its function is to protect the median caudal artery that traverses the haemal arch, its presence in the entire tail of the collared anteater suggests that this artery runs through the entire length of the tail. The “Y” shape of the haemal process was also described in nine-banded armadillos, diverging from the “V” shape of most armadillos⁶ and giant anteaters¹³.

Conclusion

The collared anteater shows intra- and interspecific variations compared to other Xenarthra and mammals in the vertebral count of the thoracic, lumbar, sacral, and caudal columns, the location of the xenarthrous and haemal processes, and the absence of fusion of the vertebrae from the anterior portion of the tail to the sacrum.

The low number of lumbar vertebrae and the absence of variation in their number in relation to the number of thoracic vertebrae suggests that the last thoracic segment is the source of the nerves of the lumbar plexus. Body weight support during the bipedal posture is performed only by the xenarthrous processes of the lumbar vertebrae.

References

- Machado A.B.M., Drummond G.M. & Paglia A.P. 2008. Livro vermelho da fauna brasileira ameaçada de extinção. Fundação Biodiversitas, Belo Horizonte.
- Miranda F.R. 2012. Status de conservação de tamanduás no Brasil. In: Miranda F.R. (Ed.). Manutenção de tamanduás em cativeiro. Editora Cubo, São Carlos. https://www.academia.edu/8921151/Manejo_de_Tamandu%C3%A1s_em_Cativeiro
- Miranda F., Fallabrino A., Arteaga M., Tírra D.G., Meritt D.A. & Superina M. 2014. *Tamandua tetradactyla*. The IUCN Red List of Threatened Species 2014: e.T21350A47442916. <https://doi.org/10.2305/IUCN.UK.2014-1.RLTS.T21350A47442916.en>
- Bernegossi A.M., Rahal S.C., Melchert A., Teixeira C.R., Lima F.H., Medeiros R.D. & Silva A.A. 2018. Evaluation of collared anteaters (*Tamandua tetradactyla*) presented in a wildlife health reference center of São Paulo state, Brazil. *Biota Neotrop.* 18(1):e20170440. <https://doi.org/10.1590/1676-0611-BN-2017-0440>
- Borges N.C., Cruz V.S., Fares N.B., Cardoso J.R. & Bragato N. 2017. Morphological evaluation of the thoracic, lumbar and sacral column of the giant anteater (*Myrmecophaga tridactyla* Linnaeus, 1758). *Pesq. Vet. Bras.* 37(4):401-407. <https://doi.org/10.1590/S0100-736X2017000400016>
- Alves L.S., Midon M., Filadelpho A.L. & Vulcano L.C. 2017. Gross osteology, radiographic and computed tomographic morphology of the axial skeleton of the nine-banded armadillo (*Dasypus novemcinctus*). *Anat. Histol. Embryol.* 46(2):162-177. <http://dx.doi.org/10.1111/ah.12247>
- Vizcaíno S.F. & Loughry W.J. 2008. The biology of the Xenarthra. University Press of Florida, Gainesville.
- Asher R.J., Lin K.H., Kardjilov N. & Hautier L. 2011. Variability and constraint in the mammalian vertebral column. *J. Evol. Biol.* 24:1080-1090. <https://dx.doi.org/10.1111/j.1420-9101.2011.02240.x>
- Iwanaga, J., Singh, V., Takeda, S., Ogeng'o, J., Kim, H.-J., Mory_s, J., Ravi, K. S., Ribatti, D., Trainor, P. A., Sañudo, J. R., Apaydin, N., Sharma, A., Smith, H. F., Walocha, J. A., Hegazy, A. M. S., Duparc, F., Paulsen, F., Del Sol, M., Addis, P., ... Tubbs, R. S. (2022). Standardized statement for the ethical use of human cadaveric tissues in anatomy research papers: Recommendations from Anatomical Journal Editors-in-Chief. *Clinical Anatomy*, 1-3. <https://doi.org/10.1002/ca.23849>
- Galliari F.F., Carlini A.A. & Sánchez-Villagra, M.R. 2010. Evolution of the axial skeleton in armadillos (Mammalia, Dasypodidae). *Mamm. Biol.* 75(4):326-333. <https://doi.org/10.1016/j.mambio.2009.03.014>
- Budras K. D., Mccarthy P. H., Horowitz A. & Berg R. 2007. Surface of the Body and Axial Skeleton. In: Budras K. D., Mccarthy P. H., Horowitz A. & Berg R. (Eds.) *Anatomy of the dog*. 5th.ed. Schlutersche Verlagsgesellschaft & Co., Hannover.
- Jenkins Jr. F.A. 1970. Anatomy and function of expanded ribs in certain edentates and primates. *J. Mammal.* 51(2):288-301. <https://doi.org/10.2307/1378479>
- Borges, N.C.; NARDOTTO, J. R. B. ; OLIVEIRA, R. S. L. ; RUNCOS, L. H. E. ; RIBEIRO, R. G. ; Andria de Melo Bogoevich . Anatomy description of cervical region and hyoid apparatus in living giant anteaters *Myrmecophaga tridactyla* Linnaeus, 1758. PESQUISA VETERINÁRIA BRASILEIRA (ONLINE) , v. 37, p. 1345-1351, 2017.
- Franzo V.S., Vulcani V.A.S., Artoni S.M.B., Gradela A. & Barreiro F.R. 2011. Estudo da fórmula vertebral do tatu-galinha. *Rev. Cient. Eletr. de Med. Vet.* (17): 1-7. <http://repositorio.bc.ufg.br/handle/ri/14379>
- Hayssen V. 2011. *Choloepus hoffmanni* (Pilosa: Megalonychidae). *Mamm. Species* 43(873):37-55. <https://doi.org/10.1644/873.1>
- Da Costa R.C. & Samii V.F. 2010. Advanced imaging of the spine in small animals. *Vet. Clin. N. Am.* 40:765-790. <https://doi.org/10.1016/j.cvsm.2010.05.002>
- Endo H., Hashimoto O., Taru H., Sugimura K., Fujiwara S., Itou T., Koie H., Kitagawa M. & Sakai T. 2013. Comparative morphological examinations of the cervical and thoracic vertebrae and related spinal nerves in the two-toed sloth. *Mammal Study* 38(3):217-224. <https://doi.org/10.3106/041.038.0310>
- Gaudin T.J. 1999. The Morphology of Xenarthrous Vertebrae (Mammalia: Xenarthra). *Fieldiana (Geology)*, New York.
- Frandson R.D., Wilke W.L. & Fails A.D. 2011. O sistema esquelético. In: Wilke W.L., Fails A.D. & Frandson R.D. *Anatomia fisiologia dos animais de fazenda*. 7th ed. Guanabara Koogan, Rio de Janeiro.
- Rose K.D. 2006. The beginning of the age of mammals. The Johns Hopkins University Press, Baltimore.
- Getty R. 1986. *Sisson and Grossman - Anatomia dos Animais Domésticos*. 5th ed. Editora Guanabara Koogan, Rio de Janeiro.
- Sánchez-Villagra M.R., Narita Y. & Kuratani S. 2007. Thoracolumbar vertebral number: the first skeletal synapomorphy for afrotherian mammals. *Syst. Biodivers.* 5(1):1-7. <https://doi.org/10.1017/S1477200006002258>
- Baines E.A., Grandage J., Herrtage M.E. & Baines S.J. 2009. Radiographic definition of the anticlinal vertebra in the dog. *Vet. Radiol. Ultrasound* 50(1):69-73. <https://onlinelibrary.wiley.com/doi/10.1111/j.1740-8261.2008.01492.x>
- Endo, H., Komiya, T., Kaeada, S., Hayashida, A., Kimura, J., Itou, T., Koie H. & Sakai T. 2009. Three-dimensional reconstruction of the xenarthrous process of the thoracic and lumbar vertebrae in the giant anteater. *Mammal Study* 34(1):1-6. <https://doi.org/10.3106/041.034.0101>
- Nyakatura J.A. & Fischer M.S. 2010. Functional morphology and three-dimensional kinematics of the thoraco-lumbar region of the spine of the two-toed sloth. *J. Exp. Biol.* 213(24):4278- 4290. <https://doi.org/10.1242/jeb.047647>

Mini Curriculum and Author's Contribution

- Adriana Gradela – PhD. Contribution: Effective scientific and intellectual participation for the study; dissections; data acquisition, data interpretation; preparation and draft of the manuscript. ORCID: 0000-0001-5560-6171
- Marcelo D. de Faria – PhD. Contribution: Effective scientific and intellectual participation for the study; dissections and data acquisition. ORCID: 0000-0002-3558-9842
- Alisson J. de O. Nunes – Mr. Contribution: Effective scientific and intellectual participation for the study; dissections and data acquisition. ORCID: <http://orcid.org/0000-0002-9277-557X>
- Raphaela C. Torres – Ms. Contribution: Effective scientific and intellectual participation for the study; dissections and data acquisition. ORCID: 0000-0002-1813-9604
- Fábio M. Corrêa – PhD. Contribution: Effective scientific and intellectual participation for the study; statistical analysis, data interpretation; preparation and draft of the manuscript. ORCID: 0000-0002-6708-9316

Received: August 5, 2024
Accepted: August 22, 2024

Corresponding author
Adriana Gradela
E-mail: agradela@hotmail.com